

Correlation of Optical and EPR Signals with the P460 Heme of Hydroxylamine Oxidoreductase from *Nitrosomonas europaea*[†]

David M. Arciero,[‡] Adina Golombek,[§] Michael P. Hendrich,[§] and Alan B. Hooper^{*,‡}

Department of Genetics and Cell Biology, University of Minnesota, St. Paul, Minnesota 55108, and Department of Chemistry, Carnegie Mellon University, Pittsburgh, Pennsylvania 15213

Received September 3, 1997[®]

ABSTRACT: Hydroxylamine oxidoreductase (HAO) of *Nitrosomonas europaea* catalyzes the four-electron oxidation of NH_2OH to NO_2^- . Each subunit of the trimeric enzyme contains seven *c*-hemes and one heme P460. In previous work [Hendrich, M. P., et al. (1994) *J. Am. Chem. Soc.* 116, 11961–11968], an integer-spin EPR signal at $g = 7.7$ was discovered from the active site of the resting enzyme. This new signal was assigned to an exchange-coupled cluster containing ferric heme P460 and a ferric *c*-heme. An electrochemical titration of HAO is presented here in which EPR signals and optical bands, believed to be associated with the P460 heme, are monitored. In the EPR titration, as a redox center with $E_{\text{m8}} = -140$ mV becomes reduced, the integer-spin signal disappears. Then, upon reduction of a redox center with $E_{\text{m8}} = -190$ mV, a $g = 6$ type signal, which has been previously assigned to a high-spin form of the ferric P460 heme of HAO, appears. However, in the -140 to -190 mV range, we have been unable to identify an additional EPR signal attributable to the P460 center. Thus, the electronic environment of oxidized P460 heme of HAO appears to pass through three states before reduction in a titration experiment, with an intermediate state that is not readily detectable by X-band EPR. The best candidate for the *c*-heme partner of the P460 heme is the heme at -190 mV, which would correspond to heme 6 of the crystal structure. A possible function of the exchange-coupled heme cluster is to facilitate two-electron oxidation steps of the substrate. An earlier spectropotentiometric titration of HAO [Collins, M. J., et al. (1993) *J. Biol. Chem.* 268, 14655–14662] identified a broad, weak optical band, centered near 740 nm, that was tentatively assigned to the oxidized P460 heme. This assignment has been strengthened by additional spectropotentiometric titrations at several values of pH and also by rapid kinetic experiments following the reduction of HAO by dithionite. The 740 nm band is not observed in fully oxidized HAO. In the spectropotentiometric titrations, its appearance cannot be correlated with reduction of a specific *c*-heme nor modeled to a Nernstian one-electron redox center. Instead, the range of potential in which the 740 nm band is present depends on whether the titration is carried out in an oxidative or reductive direction. One possible interpretation is that the 740 nm band is a property of the oxidized high-spin P460 heme but not of the low-spin state, and that the transition between the two spin states occurs at different potentials depending on the direction of the electrochemical titration.

Nitrosomonas europaea is an autotrophic bacterium that uses ammonia as an energy source. The pathway includes the enzyme hydroxylamine oxidoreductase¹ (HAO ; $\text{NH}_2\text{OH} + \text{H}_2\text{O} \rightarrow \text{NO}_2^- + 4\text{e}^- + 5\text{H}^+$) (1), which is believed to be

the starting point for the complex process that ultimately results in ATP synthesis and reverse electron flow necessary for reduction of NADP^+ in the organism. HAO is one of the most complex hemoproteins known. The enzyme contains eight covalently bound hemes per 63 kDa subunit, of which seven are *c*-hemes (2). The eighth heme has very unusual spectroscopic properties and is referred to as heme P460 (3) because its Soret band is observed at 463 nm after reduction. Whereas the various *c*-hemes are believed to be involved in intra- or intermolecular electron transfer, the P460 heme appears to be critical to catalytic function of HAO. Treatment of the enzyme with H_2O_2 results in loss of hydroxylamine-oxidizing activity and the selective destruction of the P460 heme (4, 5). As such, the structural and spectroscopic properties of the P460 heme have been the subject of numerous studies, and possible models have been proposed. Mossbauer spectroscopy of the reduced P460 heme of HAO reveals a quadrupole splitting (ΔE_{Q}) of 4.21 mm/s, a value unusually large for a ferrous heme protein

[†] This work was supported by Grant NSF/DMB-9019687 (A.B.H.) and Searle Scholars Programs and NIH Grant GM49970 (M.P.H.).

^{*} Author to whom correspondence should be addressed. Telephone: (612) 624-4930. Fax: (612) 625-5754. E-mail: hooper@cbs.umn.edu.

[‡] University of Minnesota.

[§] Carnegie Mellon University.

[®] Abstract published in *Advance ACS Abstracts*, December 15, 1997.

¹ Abbreviations: AMO, ammonia monooxygenase; HAO, hydroxylamine oxidoreductase; EPR, electron paramagnetic resonance; *N. europaea*, *Nitrosomonas europaea*; DBIS, 2,6-dibromoisindolylidene; DCIP, dichlorophenolindophenol; DBIG, 2,6-dibromo-3'-methoxyindophenol; PMS, phenazine methosulfate; GC, galloylamine; I4S, indigo tetrasulfonate; I3S, indigo trisulfonate; IC, indigo carmine; 26ADS, anthraquinone-2,6-disulfonate; 2AQS, anthraquinone-2-sulfonate; ST, safranin T; BV, benzyl viologen; MV, methyl viologen; OTTLE, optically transparent thin-layer electrode; MOPS, 3-(*N*-morpholino)propanesulfonic acid; NHE, normal hydrogen electrode.

but similar to that for five-coordinate Fe(II)-containing model heme compounds containing a strong anionic fifth ligand (6). Resonance Raman spectroscopy has suggested that the symmetry properties of the P460 heme are lower than those of protoporphyrin IX or chlorins and similar to those of chlorophylls and isobacteriochlorins (7). More recently, the P460 heme of HAO has been proposed to be a *c*-heme (attached at Cys229 and Cys232) that possesses a third covalent cross-link to the polypeptide chain tentatively assigned between the 5-*meso* carbon of the porphyrin and the C2 ring carbon of Tyr467 (8, 9). This covalent structure has now been confirmed in the crystal structure of HAO (10), with the refinement that the linkage actually involves the C3 ring carbon of the tyrosine. Whether the additional cross-linking is solely responsible for the unusual spectroscopic properties remains to be determined.

The eight hemes of HAO have previously been differentiated on the basis of their midpoint potentials. Optically, six *c*-hemes displaying α -band absorption maxima at 553 nm were observed with midpoint potentials at pH 7.0 of +288, -10, -162, -192, -265, and -412 mV vs NHE, one *c*-heme with an α -band at 559 nm was found with $E_{m7} = +11$ mV, and the P460 heme, with a pH-dependent midpoint potential, was observed at $E_{m7} = -260$ mV (5). Concomitant with appearance of the 463 nm band upon reduction of the P460 heme was the disappearance of a broad, weak band near 740 nm. No other optical band has been identified with the oxidized chromophore, although it was unclear whether the 740 nm band was present in the fully oxidized enzyme.

The EPR spectrum of fully oxidized HAO shows three different types of EPR signals from eight low-spin hemes assigned as follows (11–14): four bis-histidine *c*-hemes ($g_z = 3.0$), two weakly interacting hemes ($g_z = 3.4, 2.8$), and two exchange-coupled hemes giving an interger-spin resonance at $g = 7.7$.² The integer-spin resonance vanishes upon reduction or in the presence of substrates and inhibitors. Furthermore, the P460 heme has been shown to be a component of this exchange-coupled cluster in which one heme is low-spin and the other is either low-spin or a unique intermediate- or high-spin heme (14). In partially reduced HAO, previous reductive titration studies have identified a high-spin Fe³⁺ signal at $g = 6$ which appears as a *c*-heme near -190 mV becomes reduced and vanishes upon reduction of the P460 heme (12, 13). Thus, the $g = 6$ signal has been assigned to a high-spin state of oxidized P460 heme in HAO.

Here we combine optical and EPR detection methods in a reductive titration study seeking to establish the relationship between (1) the appearance of the 740 nm optical band and reduction of a specific *c*-heme(s), (2) the disappearance of the 740 nm band and appearance of the 463 nm band associated with the reduction of the P460 heme, (3) the disappearance of the $g = 7.7$ integer-spin EPR signal and reduction of a specific *c*-heme(s), and (4) the disappearance of the $g = 7.7$ signal and appearance of the $g = 6$ signal.

MATERIALS AND METHODS

Materials. HAO was prepared from *N. europaea* as described earlier (15). Mediator dyes used included 2,6-

dibromindosalicylic acid (DBIS; TCI America, Inc.; $E^{\circ} = +275$ mV), dichlorophenolindophenol (DCIP; BDH Chemicals, Ltd.; $E^{\circ} = +215$ mV), 2,6-bromo-3'-methoxyindophenol (DBIG; TCI America, Inc.; $E^{\circ} = +160$ mV), phenazine methosulfate (PMS; Sigma Chemical (St. Louis, MO); $E^{\circ} = +80$ mV), galloxyaniline (GC; Sigma Chemical; $E^{\circ} = +20$ mV), indigo tetrasulfonate (I4S; TCI America, Inc. (Portland OR); $E^{\circ} = -46$ mV), indigo trisulfonate (I3S; TCI America, Inc. (Portland OR); $E^{\circ} = -80$ mV) indigo carmine (IC; BDH Chemicals, Ltd. (Poole, UK); $E^{\circ} = -125$ mV), anthraquinone-2,6-disulfonate (26ADS; Aldrich Chemical (Milwaukee, WI); $E^{\circ} = -170$ mV), anthraquinone-2-sulfonate (2AQS; Aldrich Chemical; $E^{\circ} = -230$ mV), safranine T (ST; Aldrich Chemical; $E^{\circ} = -290$ mV), benzyl viologen (BV; Aldrich Chemical; $E^{\circ} = -350$ mV), and methyl viologen (MV; Aldrich Chemical; $E^{\circ} = -430$ mV).

Spectroelectrochemistry. Spectroelectrochemistry was carried out on HAO (0.1–0.2 mM) at pH 7.0 or 8.0 in 50 mM MOPS buffer containing 0.1 M KCl using an optically transparent thin-layer electrode (OTTLE) cell as described previously (5). A complete description of the apparatus and instrumentation has been published (16). The Ag/AgCl reference electrode (Radiometer America Inc., Westlake, OH) was calibrated versus the ferrocyanide/ferricyanide couple as described elsewhere (17).

Kinetics. Reduction of HAO (7.5 μ M) by sodium hydro-sulfite (1 mM) was carried out anaerobically at room temperature in a total volume of 2.0 mL in 50 mM MOPS buffer at pH 6.0, 7.0, or 8.2 under continuous stirring. Spectra were obtained using a Hewlett-Packard model 8452A diode array spectrophotometer using their HP 89532K kinetics software package for a PC computer. Spectral data were recorded every 3 s for 20 min, and either individual wavelengths or full spectra were extracted from the data file and transferred to a spreadsheet program for plotting multiple time traces or reduced-minus-oxidized spectral subtractions. A reference wavelength was not required for baseline corrections of the 740 nm absorbance data. The 464 nm absorbance data³ were corrected by subtracting the absorbance at 482 nm (an isobestic point for the P460 heme) from the 464 nm absorbance data. To correct for the different extinction coefficients of the 464 and 740 nm optical bands, all time traces were normalized. Time traces for the 464 nm data were actually plotted as $\text{Abs}(482 \text{ nm}) - \text{Abs}(464 \text{ nm})$ so that all or traces, during the P460 heme reductive phase, would decrease with time.

EPR Poises. Samples of HAO (0.45 mM) for EPR were poised in two separate series. All samples were prepared in 0.1 M MOPS, pH 8.0, buffer containing 0.1 M KCl, and all dyes were at a concentration of 0.1 mM. Sodium hydro-sulfite and potassium ferricyanide were used as reductant and oxidant, respectively. In the first series, poises of +395, +3, -77, +144, and +360 mV were prepared in succession, using a contribution of DBIS, DBIG, GC, and I3S as redox mediators. The second series of samples included the poises at -78, -122, -150, -180, -209, -240, -268, -299,

² EPR signals from centers having integral spin do not obey the standard resonance condition $h\nu = g\beta B$. The use of an apparent g -value serves only as a marker and does not convey physical significance.

³ An apparent discrepancy occurs with reference to the Soret absorption band of the P460 heme as opposed to data collected at 464 nm. Data for the 463 nm band of the P460 heme of HAO is collected and reported at 464 nm, since resolution of our spectrophotometer is 2 nm (at even-numbered values).

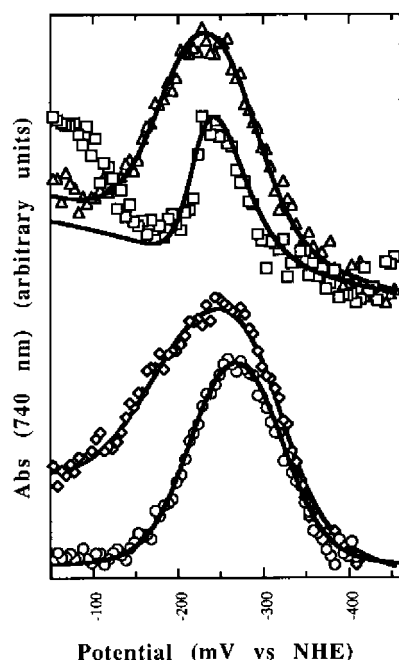


FIGURE 1: Spectroelectrochemical titrations of HAO followed at 740 nm. Potentiometric titrations of HAO at pH 7.0 (upper traces) and 8.0 (lower traces) were carried out using an optically transparent thin-layer electrode (OTTLE) cell in both the oxidative (Δ , \Diamond) and reductive (\square , \circ) directions as described in Materials and Methods. Optical spectra were obtained at 5 mV increments, and the absorbance at 740 nm was extracted from the spectra, and plotted vs potential. Theoretical curves using the Nernst equation for two separate redox centers were constructed to overlay the data using the parameters presented in Table 1. Additional details are described in the Results.

−329, and −358 mV, using a combination of I3S, IC, 26ADS, 2AQS, ST, and BV as redox mediators. The poisoning was carried out anaerobically and at room temperature in a round-bottomed flask modified by the addition of three additional ports, to accommodate reference and platinum electrodes and transfer syringes, and a well at the bottom to hold the sample. The potential was measured using an Escort EDM-1341 Digital Multimeter. The solution was stirred continuously, and the system was allowed to equilibrate for at least 20 min between additions of reductant or before a 0.25 mL sample was removed for transfer to an anaerobic EPR tube. The potential of the reference electrode was found have drifted 7 mV during the course of preparing the second series of samples. The drift was assumed to be linear over time, and the measured potentials of the poised samples were adjusted accordingly.

X-band EPR spectra were recorded on a Bruker ER300 spectrometer equipped with an Oxford ESR-9 liquid helium cryostat and a Bruker dual mode resonator (ER4116). All spectra were obtained under nonsaturating conditions. The magnetic field was calibrated with an NMR gaussmeter, and the microwave frequency was measured with a counter.

RESULTS

Optically-Monitored Potentiometric Titration of HAO. Reductive and oxidative titrations of HAO were carried out at pH values of 7.0 and 8.0. Absorbance at 740 nm between −400 mV and −50 mV is shown in Figure 1. Theoretical fits to the optical data (solid lines in Figure 1 overlaying the data points) were constructed using a two-center Nernst

Table 1: Parameters Used To Construct Theoretical Fits to Spectroelectrochemical Titrations of HAO^a

	E_m' (1) (n)	E_m' (2) (n)	baseline slope (y-intercept)
pH 7.0; R \rightarrow O	−218 mV (2)	−260 mV (1)	0.0007 (0.35)
pH 7.0; O \rightarrow R	−180 mV (1)	−280 mV (1)	0.0009 (0.45)
pH 8.0; R \rightarrow O	−215 mV (1)	−320 mV (1)	0.0000 (0)
pH 8.0; O \rightarrow R	−170 mV (0.75)	−320 mV (1)	0.0008 (0.35)

^a Solid lines in Figure 1 were constructed from the data in this table with each being comprised of two Nernstian redox centers indicated by E_m' (1) and E_m' (2), and a sloping base line.

equation, where the reduction of one gives rise to the optical band and reduction of the other results in disappearance of the band. Because of the low molar absorptivity and broad nature of the 740 nm optical band, small optical contributions were present due to other centers undergoing redox changes (dyes and *c*-hemes). These other centers precluded use of an isobestic point to improve the quality of the data. As a result, it was necessary to incorporate a linear, sloping baseline in the equation used to fit the data in three of the experiments. Additional details are as follows. The absorbance of each reduced redox center used to construct a theoretical curve was normalized to a value of 1. Upon summing the data from two opposing theoretical Nernstian centers, the maximum intensity of the expected 740 nm absorbance depended on the midpoint potentials of the two theoretical redox centers. Hence, the experimental data was first normalized between 0 and 1 and then multiplied by the maximum absorbance predicted from the theoretical fit in order to overlap the data correctly. The validity of this approach was checked by comparing these values to the maximum intensity of the raw data normalized by total 552 nm absorbance. The two sets of numbers were within 20% of each other. Parameters used to construct the theoretical fits to the data are in Table 1. Additionally, optical spectra (not shown) showed that the 740 nm optical band was absent in both fully oxidized and fully reduced HAO, was only present at intermediate potentiometric poises of HAO, and had an identical shape in all four experiments. The band also disappeared concomitant with the appearance of the 463 nm band associated with the reduced P460 heme as previously described (5).

Kinetic Analysis of Reduction of HAO by Dithionite. The optical band centered near 740 nm could also be detected transiently during reduction of HAO by dithionite, although previous studies (18) had not noted this optical band. Figure 2 shows the absorbance, as a function of time, at 740 nm (data points) and 464 nm (solid lines) following addition of dithionite to HAO. The 464 nm data in Figure 2 has been normalized to the same amplitude observed for the 740 nm data and has been plotted as if it is decreasing, rather than increasing, so as to more easily compare the time-dependent changes at the two wavelengths. The rate of reduction of hemes of HAO by dithionite has previously been shown to be pH dependent. This dependence of pH was clearly evident in the absorbance data at 464 nm, representing reduction of the P460 heme of HAO. The 740 nm band also showed a strong pH dependence as well. Significantly, at all three pH values, the disappearance of the 740 nm band followed the same kinetics as the appearance of the 463 nm band. The 464 and 740 nm data do not appear to directly

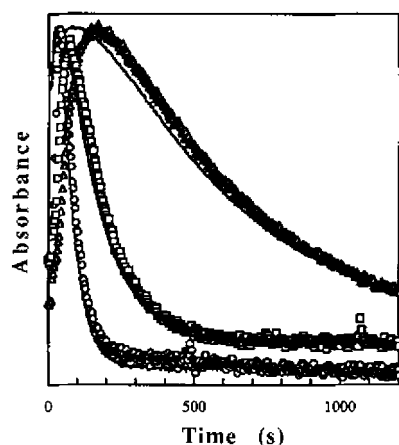


FIGURE 2: Kinetics of reduction of HAO by dithionite followed at 740 and 464 nm. HAO ($7.5 \mu\text{M}$) was reduced anaerobically with dithionite (1 mM), and optical spectra (from 434 to 820 nm) were obtained every 3 s between $t = 2$ s and $t = 1200$ s. The absorbance at 740 nm (data points) and 464 nm (plotted as $A_{482} - A_{464}$) (solid lines) was extracted, normalized, and plotted vs time. The reduction was carried out at pH 6.0 (\circ), 7.0 (\square), and 8.2 (\triangle) in 50 mM MOPS buffer.

overlay each other because the full absorbance at 740 nm is not observed, whereas the full change at 464 nm is accounted for in the time traces. This is because the 463 nm band began to appear before the 740 nm band was fully developed as in the potentiometric titrations. The *c*-hemes in HAO also showed a slight decrease in absorbance at 740 nm, as they were reduced. This accounts for the slight difference in baselines for the fully oxidized and fully reduced enzyme apparent in the 740 nm time traces. Since this is a kinetic experiment the difference is not really known, and no attempt has been made to compensate for the differing relative amounts of the two optical bands.

A series of difference spectra taken during the reduction of HAO at pH 8.2 (Figure 3) shows the optical changes at 740 nm as the band first appears (Figure 3A), and then disappears (Figure 3B) as the reduction of HAO progresses. The spectral window shown includes changes observed in the 740 nm band, the 463 nm band of the P460 heme, and the α - and β -bands of some (but not all) of the *c*-hemes. Reduction of several *c*-hemes of HAO occurred very rapidly and most of the optical changes associated with their reduction are not represented in these difference spectra. Otherwise the figures would be dominated by the α - and β -bands of *c*-hemes, making it more difficult to focus on the 740 nm band itself. The "oxidized" samples used for the subtractions in Figure 3A had the equivalent of four *c*-hemes already reduced (three *c*553 and one *c*559 hemes). The oxidized sample used for the subtractions in Figure 3B had the equivalent of about one *c*-heme still oxidized (a *c*553 heme). As can be seen in the spectra of Figure 3B, this last oxidized *c*-heme of HAO reduces faster than the P460 heme at pH 8.2. The P460 heme can be clearly seen reducing during the final stages of the reduction represented by the difference spectra of Figure 3B. The broad decrease occurring around 460 nm in Figure 3A is associated with reduction of *c*-hemes.

EPR-Monitored Potentiometric Titration of HAO. EPR spectra of poised samples of HAO at representative potentials are shown in Figure 4. The dependence of the intensities of the $g = 6$ signal and the integer-spin signal at $g = 7.7$

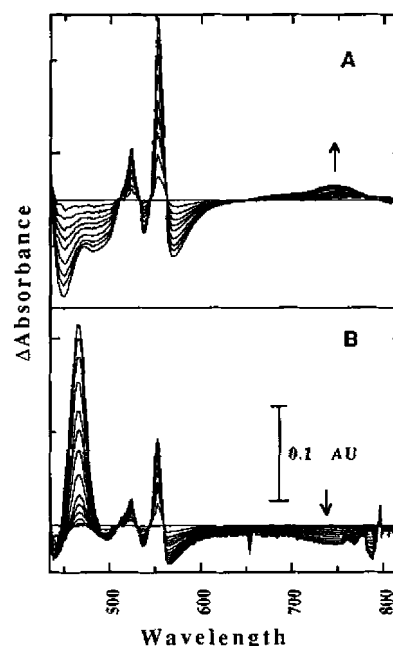


FIGURE 3: Difference spectra obtained during reduction of HAO by dithionite at pH 8.2. Spectra used are those from the experiment at pH 8.2, described in Figure 2. (A) Spectrum of HAO obtained 22 s after addition of dithionite has been subtracted from subsequent spectra obtained 28, 34, 40, 46, 52, 64, 76, 88, and 106 s after addition of dithionite. (B) Spectrum of HAO obtained 130 s after addition of dithionite has been subtracted from subsequent spectra obtained 160, 190, 220, 250, 280, 346, 421, 496, 571, 706, 856, 1006, and 1156 s after addition of dithionite. As a result, all optical features are changing relative to the flat baselines.

are shown in Figure 5. Each of these signals was described previously but had not been correlated with each other. The solid lines overlaying the data of Figure 5 are theoretical fits, assuming all are standard $1e^-$ Nernstian redox centers. For ease of comparison, the intensity of the $g = 7.7$ signal has been plotted as the fraction lost $[(1 - I)/I_{\text{max}}]$ as the potential is decreased. The $g = 7.7$ center behaved very well as a standard $1e^-$ Nernst center with $E_m' = -140$ mV, very close to the value of $E_m' = -150$ mV previously reported for reduction of one of the *c*553 heme of HAO (5). Changes in the $g = 6$ signal with potential agree very well with the previously reported EPR reductive titration (13) when the shift in midpoint potential of the heme P460 with pH (5) is accounted for. The appearance and disappearance of the $g = 6$ signal followed Nernstian behavior for $1e^-$ processes. The signal appeared upon reduction of a redox center with $E_m' = -190$ mV and disappeared upon reduction of a center with $E_m' = -320$ mV.

DISCUSSION

A clearer picture is gradually emerging with respect to the structural and spectroscopic features of the catalytically essential P460 heme of HAO and some of the myriad interactions in which it is involved. One of the basic discoveries recently made is that the P460 heme is a *c*-heme covalently modified by cross-linking to a tyrosine residue (8). The cross-linking was tentatively assigned to the C2 carbon of the tyrosyl ring and the 5-*meso* heme carbon; however, the recent crystal structure of HAO (10) shows it to involve the C3 carbon of the tyrosine. In addition, a new, broad optical band centered near 740 nm had been shown

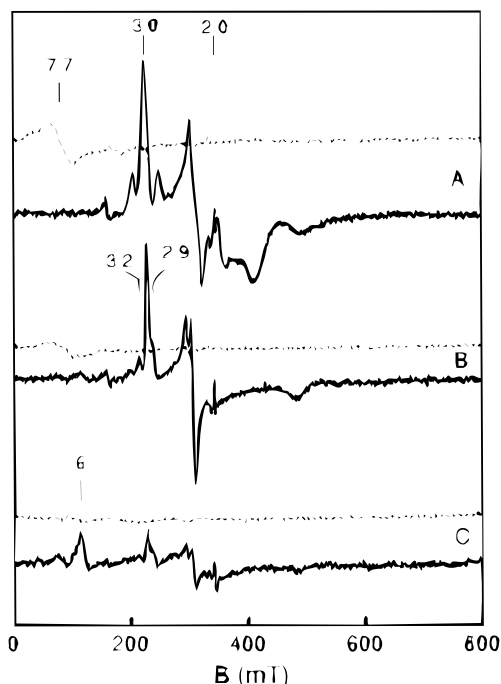


FIGURE 4: Representative parallel- (dashed line) and perpendicular-mode (solid line) EPR spectra of HAO (0.45 mM) at pH 8.0. Spectra obtained from poised samples of HAO at +395 (A), -150 (B), and -268 mV (C) vs NHE showing either the presence, appearance, or disappearance of the various EPR signals present in HAO were recorded at 20 K. All signals have been described previously. The sharp feature at $g = 2.0$ is from mediator dyes. Instrumental Parameters: $T = 20$ K; frequency = 9.64 GHz (perp), 9.32 GHz (para); power = 0.02 mW; modulation amplitude = 0.2 mT at 100 kHz.

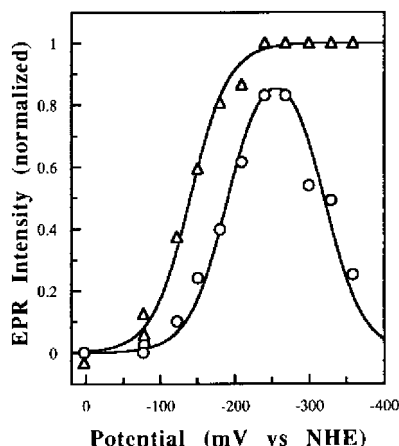


FIGURE 5: Reductive titration of EPR signals of HAO. The relative intensities (measured zero-to-peak) of the $g = 7.7$ (Δ) and $g = 6.0$ (\circ) EPR signals for a series of poised samples of HAO were plotted as a function of the poisoning potential. The solid lines represent theoretical standard Nernst curves for one-electron redox centers with $E_m' = -140$ mV for the $g = 7.7$ signal, and $E_m'(1) = -190$ mV and $E_m'(2) = -320$ mV for the $g = 6$ signal. The relative intensities of the EPR signals were normalized to the maximum intensity expected from the theoretical curves.

to disappear at the same potential at which the P460 heme became reduced (5). This was the first indication of an optical band associated with the oxidized P460 heme of HAO. Lastly a detailed EPR study revealed the existence of a new resonance in the fully oxidized enzyme which originates from an exchange-coupled iron center containing the P460 heme and vanishes in the presence of substrates

and inhibitors (14). The present study revisits these optical and EPR spectroscopic signals and attempts to correlate them with each other.

740 nm Optical Band. Here, the disappearance of the 740 nm optical band correlated well with appearance of the 463 nm band in all four electrochemical titrations,⁴ and the data followed Nernstian behavior for one-electron processes. Since appearance of the 463 nm band is firmly established with reduction of the P460 heme of HAO, the strong correlation of the two optical bands, especially in conjunction with the underlying pH dependence of the signals, provides very strong evidence that the 740 nm band is a feature of an oxidized form of the P460 heme. The appearance of the optical band, however, could not be unambiguously tied to reduction of any of the *c*-hemes in HAO since the potential at which it appears clearly depends on whether the titration is carried out reductively or oxidatively. This is in sharp contrast to what is found when other redox centers are monitored. *c*-Hemes, when monitored either at the Soret or the α -band, show no differences based on the direction of the titration. Of course, spectropotentiometric titrations would not ascertain whether midpoint potentials of two or more *c*-hemes have simultaneously moved in opposite directions, although EPR results would suggest that this is not the case. The increase in absorbance at 740 nm with potential is, for unknown reasons, also difficult to model to a single Nernstian process. It is clear that the process is essentially pH independent.

The kinetics of reduction of HAO by dithionite has been shown to be very complex with multiple rate constants observed (18) when *c*-hemes are monitored. Fortunately, monitoring individual chromophores is much simpler. The results presented here show that disappearance of the 740 nm band and appearance of the 463 nm band correlate kinetically as well as thermodynamically and show the same dependence on pH.

EPR Titration. In the potentiometric titration of HAO at pH 8, the sequence at which EPR signals known to be associated with the P460 heme appear and disappear is readily discernible. The integer-spin signal disappears with a midpoint potential of -140 mV, a value which is close to the midpoint potential of a *c*-heme at -150 mV. The integer-spin signal has been assigned to an exchange-coupled pair of Fe^{3+} hemes in which one heme is low-spin and the other is either low-spin or a unique intermediate- or high-spin heme. The disappearance of the integer-spin signal at -140 mV suggests that the -150 mV *c*-heme interacts with the active site of the HAO; however, we do not believe that the -150 mV *c*-heme is exchange-coupled to the P460 heme. No new signals are observed to grow in concomitantly with loss of the integer-spin signal as the potential is lowered between -150 and -190 mV, thus the P460 heme must

⁴ Since the 740 nm band is not present in either fully oxidized or fully reduced HAO but is only present at intermediate potentials, some confusion can arise when talking about the actual appearance and disappearance of this band. Technically, in oxidative titrations the band appears as the P460 heme is oxidized and disappears at a higher poisoning potential. The situation is reversed in reductive titrations. Hence, to avoid the confusion, the direction of the titration is ignored and the 740 nm optical band is discussed as appearing at the higher temperature potential and disappearing at the lower potential (where the P460 heme is reduced).

remain exchange-coupled in this potential range but in a new environment. At a midpoint potential of -190 mV, another heme is reduced and simultaneously a $g = 6$ signal is now observed from a high-spin Fe^{3+} state of the P460 heme. Disappearance of the $g = 6$ signal occurs at a midpoint potential of -320 mV (pH 8), showing the expected shift from -260 mV (pH 7) for the P460 heme at higher pH, predicted by previous spectropotentiometric titrations.

Earlier EPR titrations of HAO noted the appearance and subsequent disappearance of a new pair of EPR signals at $g_z = 3.2$ and 2.9 in the same intermediate potential range identified here as triggering changes in EPR signals associated with the P460 heme. However, we have found that the appearance of this pair of signals occurs at a potential higher than E_{m8} for disappearance of the $g = 7.7$ resonance.⁵ The signal intensity of the $g = 3.2, 2.9$ pair remains relatively constant in the range over which the $g = 7.7$ resonance disappears, but it never accounts for more than 0.5 total spin. The $g = 3.2, 2.9$ pair, however, disappears at an E_{m8} close to the E_{m8} for appearance of the $g = 6$ signal. We currently cannot explain the origin of the $g = 3.2, 2.9$ pair in terms of known redox changes associated with HAO. Thus, while the signals are present in the potential range between which known changes in the electronic environment of heme P460 are occurring, we cannot determine that they arise from a weakly-coupled P460 heme.

These results indicate that the P460 heme is in at least three different electronic environments in the reductive titration prior to P460 heme reduction. Reduction of the -150 mV *c*-heme triggers a change in the exchange-coupled cluster composed of the P460 and the -190 mV hemes. This change could be either a spin-state transition of the P460 heme from $S = 1/2$ to $S = 3/2$ or $5/2$ or possibly a switch in the sign of the exchange coupling, both of which could render the resulting spin system unobservable with X-band EPR. The possibility that a spin-state change occurs at -150 mV in the P460 heme is supported by the appearance of the 740 nm optical band at a similar potential of -170 mV. The third state of the oxidized P460 heme occurs at -190 mV, when the $S = 5/2$ P460 heme becomes observable as the $g = 6$ signal due to reduction of the -190 mV heme to an $S = 0$ spin state.

From the crystal structure of HAO, we can surmise that its nearest neighbor, heme 6, is the *c*-heme exchange-coupled to the P460 heme. Thus, heme 6 would have a midpoint potential of -190 mV. Heme 7 or 5 is the most likely candidate for the redox center at -150 mV which triggers the change in the exchange-coupled heme P460–heme 6 pair. Both hemes 5 and 7 are capable of interacting directly with heme 6, heme 7 through weak edge-to-edge contact of porphyrin rings, and heme 5 through an interaction involving the axial ligand of heme 6 and the porphyrin periphery of heme 5 due to the perpendicular arrangement of the two hemes. It is also possible that the -150 mV heme is one of the other *c*-hemes in HAO, and that its reduction influences the exchange-coupled heme P460–heme 6 pair through a global conformational change in HAO.

Possible Sources of the 740 nm Optical Band. The one optical feature clearly associated with the P460 heme of HAO is the 463 nm band, arising from the reduced chromophore, that defines the P460 heme. Direct observation of an optical band for the oxidized chromophore has not been reported, although suicide inactivation of HAO by hydrogen peroxide and alkyl hydrazines (19) results in a decrease in absorbance near 410 nm and thus suggests that the oxidized chromophore does indeed have a Soret band as well. Other optical features such as α, β -bands appear to be absent, however, or at least do not change upon reduction. This is in contrast to what is observed for the P460 heme of cytochrome P460 (20), a monoheme cytochrome from *N. europaea* that appears to have a lysine cross-linked to the porphyrin instead of a tyrosine (21). Reduction of cytochrome P460 results in an increase in absorbance near 690 nm but no change in absorbance at 740 nm upon reduction (22).

Since the evidence indicates that the P460 heme undergoes its spin-state change prior to its reduction, the 740 nm band must be an optical feature of the oxidized high-spin P460 center. The question is whether the 740 nm band is also a property of the exchange-coupled cluster which exhibits the integer-spin EPR signal. The OTTLE experiments are not clear on this point. The spectropotentiometric results do not clearly pinpoint the potential at which the optical band appears, and the observed potentials are midway in between the potential at which EPR signal changes occur. Since the result depends on whether the OTTLE titration is carried out reductively or oxidatively, the answer may lie in whether the poised EPR samples reflect either the oxidative or reductive titration. One possible interpretation is that the 740 nm band is a property of the oxidized high-spin P460 heme but not of the state identified with the integer-spin EPR signal. In this case, the appearance would not correlate with a thermodynamically-controlled change in redox state of a heme center but with a kinetically-controlled spin-state transition of the P460 heme. Nernstian behavior would not be expected, whereas hysteresis between a high-spin to low-spin vs a low-spin to high-spin would be more likely.

Another unresolved question regarding the 740 nm band is whether its loss as the P460 heme becomes reduced is due to a change in oxidation state of the Fe, protonation of the group that is responsible for the pH dependence of E_m' of the P460 heme, or a structural change in or near the P460 heme.

Functional Implications. Two possible intramolecular electron-transfer pathways from the active site are evident in the crystal structure of HAO. Based on the pairing of *c*-hemes in double-heme clusters, it has been proposed that HAO is capable of transferring two electrons at the same time (dielectron transfer) (10). The results presented here have some bearing on this hypothesis. The exchange-coupled heme cluster at the active site of HAO could facilitate two-electron oxidation steps of the substrate (14). However, it is harder to imagine that dielectron transfer continues through HAO since none of the other *c*-hemes behave as if they are interacting with each other, except for the weakly coupled pair with values of E_m' near 0 mV. For the other double-heme clusters to be involved in dielectron transfer, one would expect that the pairs of hemes would have identical redox potentials or that positive cooperativity between hemes existed such that the slope of the Nernst

⁵ The signals may appear as the pair of *c*-hemes with values of E_m' around 0 mV become reduced. However, insufficient data exists to accurately pinpoint E_m' for their appearance.

equation reflected two electrons being transferred. Clearly this is not the case in these or earlier titrations (5, 12, 13).

If the P460 heme-heme 6 pair act as a two-electron acceptor and all the other *c*-hemes act as one-electron carriers, HAO may have evolved a novel process of splitting electrons from a two-electron acceptor into single-electron entities without the use of flavins or quinones. However, HAO contains another pair of weakly interacting hemes that are not associated with the active site. These hemes have similar reduction potentials near 0 mV, and thus may provide HAO with a means of transfer and storage of two electrons from the active site. A second two-electron N-oxidation step can closely follow to generate nitrite and decrease possible side reactions from otherwise long-lived intermediates.

REFERENCES

1. Hooper, A. B., and Nason, A. (1965) *J. Biol. Chem.* 240, 4044–4057.
2. Arciero, D. M., and Hooper, A. B. (1993) *J. Biol. Chem.* 268, 14645–14654.
3. Erickson, R. H., and Hooper, A. B. (1972) *Biochim. Biophys. Acta* 275, 231–244.
4. Hooper, A. B., and Terry, K. R. (1977) *Biochemistry* 16, 455–459.
5. Collins, M. J., Arciero, D. M., and Hooper, A. B. (1993) *J. Biol. Chem.* 268, 14655–14662.
6. Andersson, K. K., Kent, T. A., Lipscomb, J. D., Hooper, A. B., and Munck, E. (1984) *J. Biol. Chem.* 259, 6833–6840.
7. Andersson, K. K., Babcock, G. T., and Hooper, A. B. (1991) *Biochem. Biophys. Res. Commun.* 174, 358–363.
8. Arciero, D. M., Hooper, A. B., Cai, M., and Timkovich, R. (1993) *Biochemistry* 32, 9370–9378.
9. Sayavedra-Soto, L. A., Hommes, N. G., and Arp, D. J. (1994) *J. Bacteriol.* 176, 504–510.
10. Igarashi, N., Moriyama, H., Fujiwara, T., Fukumori, Y., and Tanaka, N. (1997) *Nat. Struct. Biol.* 4, 276–284.
11. Vickery, L. E., and Hooper, A. B. (1981) *Biochim. Biophys. Acta* 670, 291–293.
12. Lipscomb, J. D., and Hooper, A. B. (1982) *Biochemistry* 21, 3965–3972.
13. Prince, R. C., and Hooper, A. B. (1987) *Biochemistry* 26, 970–974.
14. Hendrich, M. P., Logan, M., Andersson, K. K., Arciero, D. M., Lipscomb, J. D., and Hooper, A. B. (1994) *J. Am. Chem. Soc.* 116, 11961–11968.
15. Arciero, D. M., Balny, C., and Hooper, A. B. (1991) *Biochemistry* 30, 11466–11472.
16. Arciero, D. M., Hooper, A. B., and Collins, M. J. (1994) *J. Electroanal. Chem.* 371, 277–281.
17. Silva, K. E., Elgren, T. E., Que, L., Jr., and Stankovich, M. E. (1995) *Biochemistry* 34, 14093–14103.
18. Hooper, A. B., Tran, V. M., and Balny, C. (1984) *Eur. J. Biochem.* 141, 565–571.
19. Logan, M. S. P., and Hooper, A. B. (1995) *Biochemistry* 34, 9257–9264.
20. Erickson, R. H., and Hooper, A. B. (1972) *Biochim. Biophys. Acta* 275, 231–244.
21. Arciero, D. M., and Hooper, A. B. (1977) *FEBS Lett.* 410, 457–460.
22. Numata, M., Saito, T., Yamazaki, T., Fukumori, Y., and Yamanaka, T. (1990) *J. Biochem.* 108, 1016–1021.

BI972187L